Eutectic epsilon-near-zero metamaterial terahertz waveguides

M. Massaouti,[1] A. A. Basharin,[1,2] M. Kafesaki,[1,3] M. F. Acosta,[4] R. I. Merino,[4] V. M. Orera,[4] E. N. Economou,[1,5] C. M. Soukoulis,[1,6] and S. Tzortzakis[1,3,*]

[1]*Institute of Electronic Structure and Laser (IESL), Foundation for Research and Technology—Hellas (FORTH), P.O. Box 1527, Heraklion GR-71110, Greece*

[2]*National Research University "Moscow Power Engineering Institute", Moscow 112250, Russia*

[3]*Department of Materials Science and Technology, University of Crete, Heraklion GR-71003, Greece*

[4]*Instituto de Ciencia de Materiales de Aragón, CSIC-Universidad de Zaragoza, Zaragoza E-50009, Spain*

[5]*Department of Physics, University of Crete, Heraklion GR-71003, Greece*

[6]*Ames Laboratory-USDOE, and Department of Physics and Astronomy, Iowa State University, Ames, Iowa 50011, USA*

**Corresponding author: stzortz@iesl.forth.gr*

Received January 3, 2013; accepted February 15, 2013;
posted March 4, 2013 (Doc. ID 182146); published March 29, 2013

We present and analyze the unique phenomena of enhanced THz transmission through a subwavelength LiF dielectric rod lattice embedded in an epsilon-near-zero KCl host. Our experimental results in combination with theoretical calculations show that subwavelength waveguiding of terahertz radiation is achieved within an alkali–halide eutectic metamaterial as result of the coupling of Mie-resonance modes arising in the dielectric lattice.

OCIS codes: 160.3918, 130.5296, 190.7110, 300.6495.

In recent years, man-made materials, known as metamaterials, have drawn extensive attention due to their unique electromagnetic properties, such as negative permittivity/permeability, negative index of refraction, giant chirality, etc. [1–3]. Recently, particular interest is noted in the so-called epsilon-near-zero (ENZ) metamaterials, which possess a number of intriguing properties associated with the near-zero permittivity they exhibit [4–6]. Among these properties are their ability to "squeeze" electromagnetic waves (E/M) in ultranarrow ENZ channels [7], to shape the radiation phase pattern of arbitrary sources [8], to control leaky wave radiation from waveguides made by embedding defects in ENZ materials [9], etc.

ENZ metamaterials at a particular frequency can be synthesized by embedding suitable inclusions in a host medium. However, in the THz regime, which is a very challenging and appealing regime of the electromagnetic spectrum in terms of technological applications [10,11], metamaterials are not the only resort of ENZ response. Natural materials showing near-zero or small negative permittivity values already exist in this region of the E/M spectrum, known as polaritonic materials or crystals [12].

Recently it has been shown that alkali–halide polaritonic materials can be structured easily in the μm scale, using eutectics self-organization, an approach which involves well-established crystal growth procedures and can be used for an easy and large scale production [13,14]. Such an approach has been followed by A. Reyes-Coronado *et al.* for achieving polaritonic metamaterial structures in which one can obtain hyperbolic dispersion relations, showing the potential of subwavelength resolution THz imaging [15,16]. In addition, recent theoretical studies demonstrated backward-radiation-based imaging in polaritonic LiF rods embedded in either the KCl or NaCl polaritonic host, operating in the THz regime [17].

In this Letter we demonstrate, both experimentally and theoretically, enhanced transmission and subwavelength guiding and propagation of THz waves through self-organized eutectic systems made of a LiF rod lattice in a KCl host, exploiting the ENZ response of the polaritonic KCl.

According to a recent theoretical study [18] an enhancement of E/M wave transmission through an ENZ material is expected if dielectric cylinders are embedded in it. This enhanced transmission has a resonant character and it is associated with the occurrence of subwavelength Mie resonances in the cylinders which exhibit electrical permittivity much higher than the permittivity of the surrounding ENZ medium [19]. In a periodic system of such cylindrical particles (photonic lattice), the resonances of the nearby particles are combined to give a transmission band, in the same way that the atomic orbitals are combined to give a propagation band for electrons in a tight-binding scheme.

In the case of the LiF/KCl system, the electrical permittivity of both LiF rods and KCl host obey a resonant response of Lorenz type [12], giving ENZ for frequencies $\omega \sim \omega_L$, where ω_L is the angular frequency of longitudinal optical phonons of the material. In particular, the KCl host ($f_L = \omega_L/2\pi = 6.196$ THz) shows an ENZ response around 6 THz, ($\varepsilon_{\mathrm{KCl}} \sim 0$), while the LiF in the frequency range between 4 THz up to 8 THz exhibits positive permittivity, i.e., dielectric-like response [16], with $\varepsilon_{\mathrm{LiF}} = 15.5$ at ~6 THz.

In order to fabricate the LiF/KCl eutectic samples studied here, the directional solidification technique has been followed, using the Bridgman method [20], where LiF and KCl powders of high purity are mixed in their eutectic composition: 91% KCl and 9% LiF by weight, respectively. The geometrical features of the produced LiF/KCl eutectic metamaterials are shown in Figure 1(c). In the resulting crystals, the single crystalline LiF rods are placed in an almost hexagonal lattice arrangement, as shown in Fig. 1(b), with approximate filling ratio

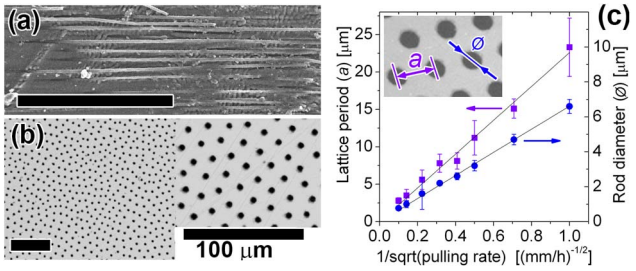

Fig. 1. (Color online) (a) Scanning electron microscopy (SEM) image of a polished longitudinal cross section of the eutectic LiF/KCl partially corroded by ambient humidity. The brighter long fibers are the long continuous, single crystalline LiF rods forming the lattice embedded in the KCl matrix. (b) SEM image of the transverse cross section of LiF/KCl eutectic sample grown at 2 mm/h pulling rate. The dark phase in (b) is LiF. (c) Size of the microstructural features of LiF/KCl eutectic samples. In (a) and (b), the scale bars are 100 μm long.

6.95% and lattice constant and rod radius depending on the rate of solidification (pulling rate).

Longitudinal slices (i.e., parallel cuts to the rod axes) of LiF/KCl eutectics grown at 2 mm/h pulling rate (resulting in 4.2 μm rod diameter and 15.1 μm lattice period) were studied in the region 0.4–8 THz, using a THz time domain spectroscopic system (THz–TDS). The system is based on a pump-probe, coherent detection approach, and uses an amplified kHz Ti:Sa laser system delivering 35 fs pulses at 800 nm central wavelength and maximum energy of 2.3 mJ/pulse. Intense THz pulses, of maximum field 200 kV/cm, are produced through 2-color filamentation in air and their detection is achieved following the standard time-resolved electro-optic sampling method using a 100 μm thick GaP crystal [21].

In Fig. 2(a), we present the frequency-dependent amplitude T of the transmitted THz pulse through the eutectic material as retrieved by the normalized sample spectrum, using as reference the THz electric field in absence of any sample. The two different spectra in Fig. 2(a) correspond to parallel polarization (black-circles), i.e., incident electric field parallel to the LiF rods, and perpendicular polarization (purple-triangles). As one can clearly see, in the case of perpendicular polarization, the eutectic system exhibits zero transmission ($T = 0.05\%$) between 4.3 and 6.2 THz, corresponding to 48–70 μm, while it maintains a high transmittance

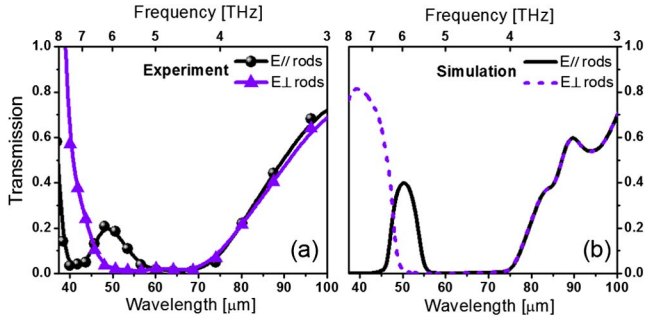

Fig. 2. (Color online) (a) THz transmission spectra, through a 60 μm thick, LiF/KCl system, as recorded for a polarization of the THz electric field parallel (circles) and perpendicular (triangles) to the LiF rods lattice, (b) THz transmission through the sample as simulated using the CST Microwave studio.

in the rest of the THz region. Interestingly, for parallel polarization, a transmission peak (20%) appears centered around the frequency of 6 THz, close to the frequency where the KCl host presents ENZ response.

As was recently shown theoretically [18], for parallel polarization the transmission amplitude through a dielectric subwavelength cylinder (like our LiF rods) embedded in an ENZ host (KCl) shows a sharp resonance, leading to even total transmission, when the condition $J_0(k_2R) = 0$ is fulfilled, with J_0, the zeroth-order cylindrical Bessel function; $k_2 = k_0\sqrt{\varepsilon\mu}$, $k_0 = \omega/c$ and ε, μ the relative permittivity and permeability of the cylinder, respectively; and R the cylinder radius. This condition is fulfilled when the incident wave frequency is close to the frequency of a Mie-resonance mode of the cylinder (for the first resonance $k_2R \sim 2.4$). In cases where more than one dielectric cylinders are present in an ENZ host, the condition for maximum transmission is practically the same as in the one cylinder case, with the only difference being the widening of the respective transmission peaks due to coupling between nearby cylinders.

In Fig. 2(b), we present the numerically calculated (using CST Microwave Studio) transmission amplitude through a hexagonal lattice of LiF rods in a KCl matrix, with rod diameter and lattice period as in the experimentally characterized system, and taking for system length along the propagation direction 6 unit cells. In agreement with the experimental observations, for perpendicular polarization (dotted purple line), a zero transmission through the system is predicted within the THz frequency range from 4.0 THz up to 6.0 THz, while a resonance peak is present in the case of parallel polarization (solid–black line), centered at ~6 THz and with peak transmission amplitude $T = 40\%$. At this frequency the resonance condition ($k_2R = 2.4$), leading to total transmission, is fulfilled for $R \sim 4.8$ μm. Nevertheless, in our case, where the cylinders are of smaller radius, not total but enhanced transmission is predicted, indicating that the experimentally observed T peak is an enhanced transmission associated with Mie resonances in the LiF cylinders. The weaker transmission amplitude peak observed experimentally is mainly due to the diversity of the orientation of the LiF rods.

An additional feature characterizing the predicted resonant response is associated with an electric field which is strongly confined along the direction of the incident wave [18] (let's assume x direction), resembling the form of a p_x atomic orbital. According to these theoretical predictions, subwavelength waveguiding is expected along the x direction due to the excitation and coupling of the p_x-like modes of the neighboring along x cylinders. In a two-dimensional periodic system like the one we study here, subwavelength waveguiding along propagation direction is also expected.

This expectation is confirmed in Fig. 3, where we present the field amplitude distribution of a plane THz wave, as propagating through homogeneous KCl and LiF bulks and through a LiF/KCl microstructured system with geometrical features as in the experimentally characterized sample.

In all three cases, the system is excited by a plane wave of 6 THz frequency, passing through a slit 50 μm wide (top row of Fig. 3) and 15 μm wide (bottom row of Fig. 3),

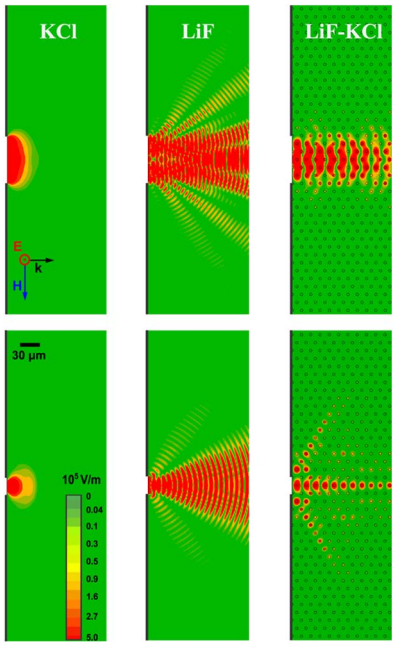

Fig. 3. (Color online) The electric field amplitude distribution of a plane wave, of 6 THz frequency, propagating (left) in a pure KCl medium, (middle) in pure LiF, and (right) in a the KCl/LiF eutectic. The E/M radiation passes through a 50 μm slit (top row) and 15 μm slit (bottom row). The rod diameter and lattice period of the microstructured sample are 4.47 and 15.77 μm, respectively.

which were realized by placing a perfect electric conductor screen with a corresponding hole. We notice that the THz wave is rapidly absorbed while transmitted through a pure KCl medium while in the pure LiF medium, it is strongly diffracted (due to the hole dimensions). On the other hand, when one has the KCl/LiF eutectic, the wave is kept collimated and confined along the propagation direction. In particular, for the 50 μm slit (top row of Fig. 3), the field does not extend beyond the size of the slit in the lateral direction with attenuation losses of 0.052 dB/μm. For the subwavelength slit of 15 μm (bottom row of Fig. 3) the field is concentrated along one row of rods in the direction of propagation and weakly attenuated (0.091 dB/μm) subwavelength guiding is observed. The two additional lobes observed in the bottom row of Fig. 3 are associated with the hexagonal lattice feature and the slit width, which introduces incident wave-vectors along the direction of closely placed rods of the hexagonal lattice. Calculations, which are not presented here, have shown that in the case of a square lattice, the location of rods would lead to only one central lobe.

In conclusion, we have demonstrated experimentally enhanced transmission of THz waves through self-organized polaritonic eutectic systems of a LiF rod lattice in a KCl host associated with Mie resonances of the lattice and the ENZ response of the KCl host. The theoretical interpretation of the results verified that this transmission is associated with subwavelength waveguiding within the microstructures of the ENZ eutectic material. These results pave the way for realizing simple subwavelength waveguides in the THz regime using self-organized natural materials which, in contrast to what is usually achieved with today's metamaterials, may exhibit ENZ response for any E/M polarization and propagation direction within this region of the E/M spectrum.

We acknowledge financial support of this work from the following EU research projects: ENSEMBLE (grant no. 213669), CHARISMA (grant no. 228330), "LASERLAB-EUROPE" (grant no. 284464), Aristeia "FTERA" (grant no 2570), NIMNIL (grant no. 228637), the project ERC-02 ExEL (grant no. 6260), RFBR (grant no. 10-02-01403), REP 2009-2013 (grant no. 14.B37.21.1211), and the Ministerio de Ciencia Tecnología y Universidad (Spain) for an FPU scholarship.

References

1. J. B. Pendry, Phys. Rev. Lett. **85**, 3966 (2000).
2. C. M. Soukoulis and M. Wegener, Nat. Photonics **5**, 523 (2011).
3. P. Tassin, T. Koschny, M. Kafesaki, and C. M. Soukoulis, Nat. Photonics **6**, 259 (2012).
4. R. W. Ziolkowski, Phys. Rev. E **70**, 046608 (2004).
5. Y. Xu and H. Chen, Appl. Phys. Lett. **98**, 113501 (2011).
6. S. Enoch, G. Tayeb, P. Sabouroux, N. Guerin, and P. Vincent, Phys. Rev. Lett. **89**, 213902 (2002).
7. M. Silveirinha and N. Engheta, Phys. Rev. Lett. **97**, 157403 (2006).
8. A. Alù, M. G. Silveirinha, A. Salandrino, and N. Engheta, Phys. Rev. B **75**, 155410 (2007).
9. V. C. Nguyen, L. Chen, and K. Halterman, Phys. Rev. Lett. **105**, 233908 (2010).
10. H.-R. Park, Y.-M. Bahk, J. H. Choe, S. Han, S. S. Choi, K. J. Ahn, N. Park, Q. H. Park, and D.-S. Kim, Opt. Express **19**, 24775 (2011).
11. H. Pahlevaninezhad, B. Heshmat, and T. E. Darcie, Opt. Express **19**, B47 (2011).
12. E. D. Palik, *Handbook of Optical Constants of Solids* (Academic, 1985).
13. J. Llorca and V. M. Orera, Prog. Mater. Sci. **51**, 711 (2006).
14. D. A. Pawlak, S. Turczynski, M. Gajc, K. Kolodziejak, R. Diduszko, K. Rozniatowski, J. Smalc, and I. Vendik, Adv. Funct. Mater. **20**, 1116 (2010).
15. S. Foteinopoulou, M. Kafesaki, E. N. Economou, and C. M. Soukoulis, Phys. Rev. B **84**, 035128 (2011).
16. A. Reyes-Coronado, M. F. Acosta, R. I. Merino, V. M. Orera, G. Kenanakis, N. Katsarakis, M. Kafesaki, C. Mavidis, J. G. de Abajo, E. N. Economou, and C. M. Soukoulis, Opt. Express **20**, 14663 (2012).
17. A. A. Basharin, M. Kafesaki, E. N. Economou, and C. M. Soukoulis, Opt. Express **20**, 12752 (2012).
18. A. A. Basharin, M. Kafesaki, E. N. Economou, and C. M. Soukoulis, "Epsilon near-zero based phenomena in metamaterials," submitted to Phys. Rev. B.
19. L. Peng, L. Ran, H. Chen, H. Zhang, J. A. Kong, and T. M. Grzegorczyk, Phys. Rev. Lett. **98**, 157403 (2007).
20. V. M. Orera and Á. Larrea, Opt. Mater. **27**, 1726 (2005).
21. M. Massaouti, J. M. Manceau, A. Selimis, and S. Tzortzakis, J. Mol. Struct. **1006**, 28 (2011).